Marine and Petroleum Geology 156 (2023) 106468

Contents lists available at ScienceDirect

Marine and Petroleum Geology

journal homepage: www.elsevier.com/locate/marpetgeo

High-resolution sequence stratigraphy of clastic shelves IX: Methods for recognizing maximum flooding conditions in shallow-marine settings

Massimo Zecchin [a,*], Octavian Catuneanu [b], Mauro Caffau [a]

[a] National Institute of Oceanography and Applied Geophysics - OGS, 34010, Sgonico, TS, Italy
[b] Department of Earth and Atmospheric Sciences, University of Alberta, 1-26 Earth Sciences Building, Edmonton, Alberta, T6G 2E3, Canada

ARTICLE INFO

Keywords:
High-resolution sequence stratigraphy
Clastic shelves
High-frequency sequences
Maximum flooding surface
Downlap surface
Local flooding surface
Maximum water-depth surface

ABSTRACT

Maximum flooding conditions in high-frequency sequences are associated with a condensed section, a generally cryptic maximum flooding surface, and with facies contacts marked by grain size changes, shell beds and bioturbation; i.e., the downlap surface and the local flooding surface. Conditions of maximum water depth usually occur above the condensed section, in the early highstand systems tract. Due to its importance in sequence stratigraphic analysis, the identification of the precise position of the maximum flooding surface, which separates the transgressive and highstand systems tracts, is critical. This is particularly true in high-resolution studies based on field and core data, where only facies contacts that are older and younger than the maximum flooding surface are recognizable. An integration of several criteria, including sedimentological (facies analysis), diagenetic, micropaleontological, geophysical and geochemical, represents the best approach to define a relatively thin uncertainty interval within high-frequency sequences, in which the cryptic MFS should lie. Among the available criteria, those sedimentological and diagenetic are the ones best suited to recognize facies contacts, whereas those micropaleontological are the most reliable ones to identify the position of the maximum flooding surface. Future studies on the integration of these methods with those geophysical and geochemical have the potential to improve the ability to identify the maximum flooding surface, and improve the available tools in the high-resolution sequence stratigraphic analysis.

1. Introduction

Stages of maximum flooding in stratigraphic sequences are generally associated with deeper depositional settings, relatively fine-grained sedimentation and the development of condensed sections (Loutit et al., 1988; Galloway, 1989; Posamentier and Allen, 1999; Catuneanu, 2006, 2022) (Fig. 1). In general, these stages are linked to the maximum flooding surface (MFS, Fig. 1), which marks a shift between transgressive and normal regressive shoreline trajectories (Posamentier et al., 1988; Van Wagoner et al., 1988; Catuneanu, 2006, 2022; Zecchin and Catuneanu, 2013) and is equated with the downlap surface at the base of the highstand prograding wedge in seismic profiles (Baum and Vail, 1988) (Fig. 2). However, this simple scheme is not applicable in high-resolution studies based on outcrop and core data, as the MFS is generally cryptic and does not necessarily coincide with a downlap surface, being such surfaces usually separated by part of the condensed section (Zecchin and Catuneanu, 2013; Catuneanu, 2022) (Fig. 1). Moreover, well recognizable facies contacts in high-resolution data commonly develop before or after the maximum flooding conditions are reached, and they in general do not coincide with the MFS (Zecchin and Catuneanu, 2013; Maravelis et al., 2018; Zecchin et al., 2021, 2022a) (Fig. 1). Methods to constrain the position of the cryptic MFS in high-resolution studies are therefore needed, and they necessarily require an integration and cross-calibration of several sedimentological, diagenetic, micropaleontological, geophysical and geochemical criteria, which all present strengths and weaknesses when used independently.

This paper represents the ninth part of a series of papers aimed at reviewing the high-resolution sequence stratigraphy of clastic shelves. The previous contributions were organized as follows: units and bounding surfaces (Part I; Zecchin and Catuneanu, 2013); controls on sequence development (Part II; Catuneanu and Zecchin, 2013); applications to reservoir geology (Part III; Zecchin and Catuneanu, 2015); high-latitude settings (Part IV; Zecchin et al., 2015); criteria to discriminate between stratigraphic sequences and sedimentological cycles (Part V; Zecchin et al., 2017); mixed siliciclastic-carbonate systems (Part VI; Zecchin and Catuneanu, 2017); 3D variability of stacking

* Corresponding author
E-mail address: mzecchin@ogs.it (M. Zecchin).

https://doi.org/10.1016/j.marpetgeo.2023.106468
Received 15 June 2023; Received in revised form 16 August 2023; Accepted 17 August 2023
Available online 19 August 2023

patterns (Part VII; Zecchin and Catuneanu, 2020); full-cycle subaerial unconformities (Part VIII; Zecchin et al., 2022b). The present ninth part describes the sedimentological, diagenetic, micropaleontological, geophysical and geochemical criteria that afford the identification of maximum flooding conditions in shallow-marine high-frequency sequences. The integration of different criteria allows higher precision in placing potentially cryptic surfaces associated with maximum flooding and water deepening along basin margins, and this is the recommended approach for high-resolution sequence stratigraphic studies.

2. Surfaces associated with maximum flooding conditions

Maximum flooding conditions in high-frequency stratigraphic sequences are associated with a surface of sequence stratigraphic significance, the maximum flooding surface (MFS; Posamentier et al., 1988; Van Wagoner et al., 1988) as well as with other facies contacts and/or cryptic surfaces (see Zecchin and Catuneanu, 2013; Zecchin et al., 2021, 2022a; Catuneanu, 2022) (Figs. 1 and 3).

The MFS corresponds to the seafloor at the time of maximum shoreline transgression and marks a change between transgressive and normal regressive shoreline trajectories (for a review, see Catuneanu, 2022 and references therein) (Fig. 1). Typically, the MFS lies within the condensed section (CS, Fig. 3), which records maximum sediment starving conditions between late transgressive and earliest highstand phases and is marked by an increase in the abundance of macrofossils and relatively distal microfossils, marine hardgrounds, authigenic minerals and organic matter (Loutit et al., 1988; Zecchin et al., 2021, 2022a). The MFS is commonly cryptic, without diagnostic features that would allow its recognition in outcrops and cores (Carter et al., 1998; Zecchin and Catuneanu, 2013; Zecchin et al., 2021, 2022a). While the MFS approximates a time line along depositional dip (Fig. 3), it may be associated with a variable degree of diachroneity along strike

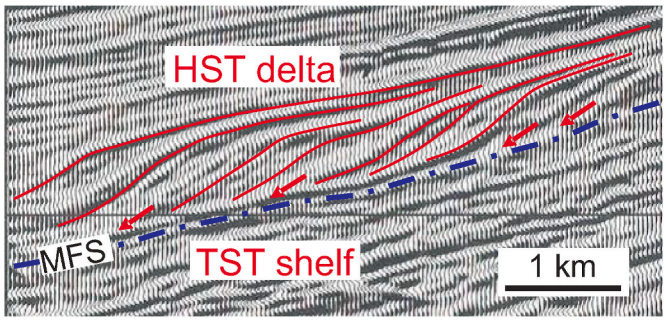

Fig. 2. Seismic profile showing a maximum flooding surface overlain by highstand clinoforms (modified from Brown et al., 1995). In low-resolution data like these, the maximum flooding surface corresponds to a downlap surface. Abbreviations: HST – highstand systems tract; MFS – maximum flooding surface; TST – transgressive systems tract.

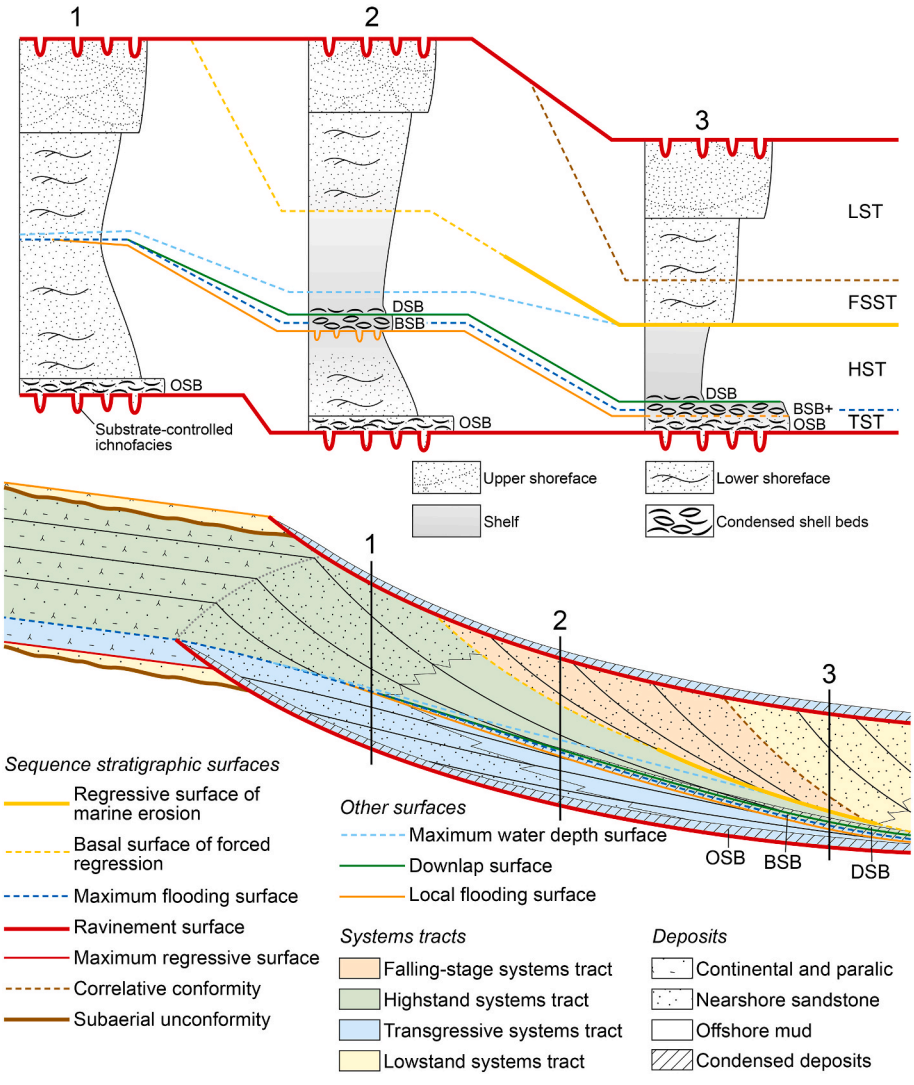

Fig. 1. Representative stratigraphic sequence bounded by two ravinement surfaces that truncate subaerial unconformities landwards (modified from Zecchin et al., 2017). Systems tracts, sequence stratigraphic surfaces and facies contacts are shown. Note the various surfaces that develop toward maximum flooding conditions. Abbreviations: BSB – backlap shell bed; DSB – downlap shell bed; FSST – falling-stage systems tract; HST – highstand systems tract; LST – lowstand systems tract; OSB – onlap shell bed; TST – transgressive systems tract.

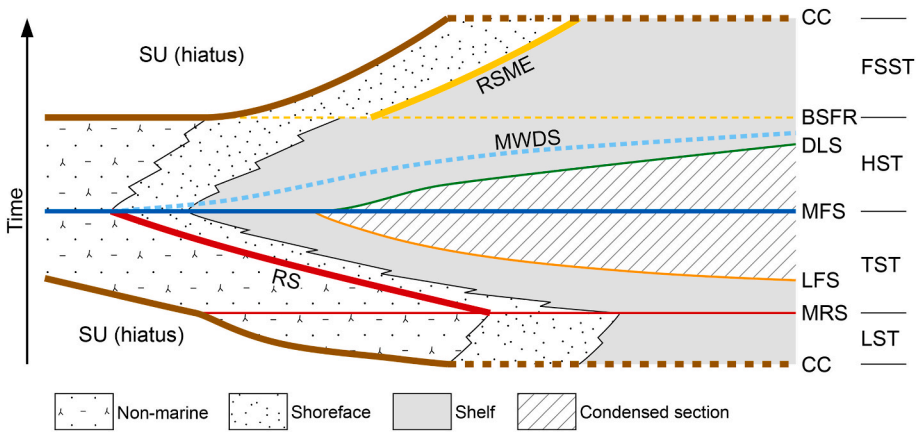

Fig. 3. Wheeler diagram showing surfaces and systems tracts developed during a full cycle or relative sea-level change (modified from Zecchin and Catuneanu, 2013; Zecchin et al., 2021). Abbreviations: BSFR – basal surface of forced regression; CC – correlative conformity; DLS – downlap surface; FSST – falling-stage systems tract; HST – highstand systems tract; LFS – local flooding surface; LST – lowstand systems tract; MFS – maximum flooding surface; MRS – maximum regressive surface; MWDS – maximum water depth surface; RS – ravinement surface; RSME – regressive surface of marine erosion; SU – subaerial unconformity; TST – transgressive systems tract.

(Catuneanu, 2006, 2022).

The local flooding surface (LFS; Abbot and Carter, 1994) is a diachronous facies contact developing on the shelf during transgression due to sediment starvation and minor erosion (Figs. 1 and 3,4,5,6); it is typically characterized by burrowing (*Glossifungites* ichnofacies; Figs. 1, 4B and 6) and marks the base of condensed skeletal accumulations (i.e., a CS) that may include community concentrations in life or near life position (the 'backlap shell bed', BSB, Kidwell, 1991; Naish and Kamp, 1997a; Kondo et al., 1998; Di Celma et al., 2005; Zecchin and Catuneanu, 2013; Zecchin et al., 2021) (Fig. 4A, 5 and 6).

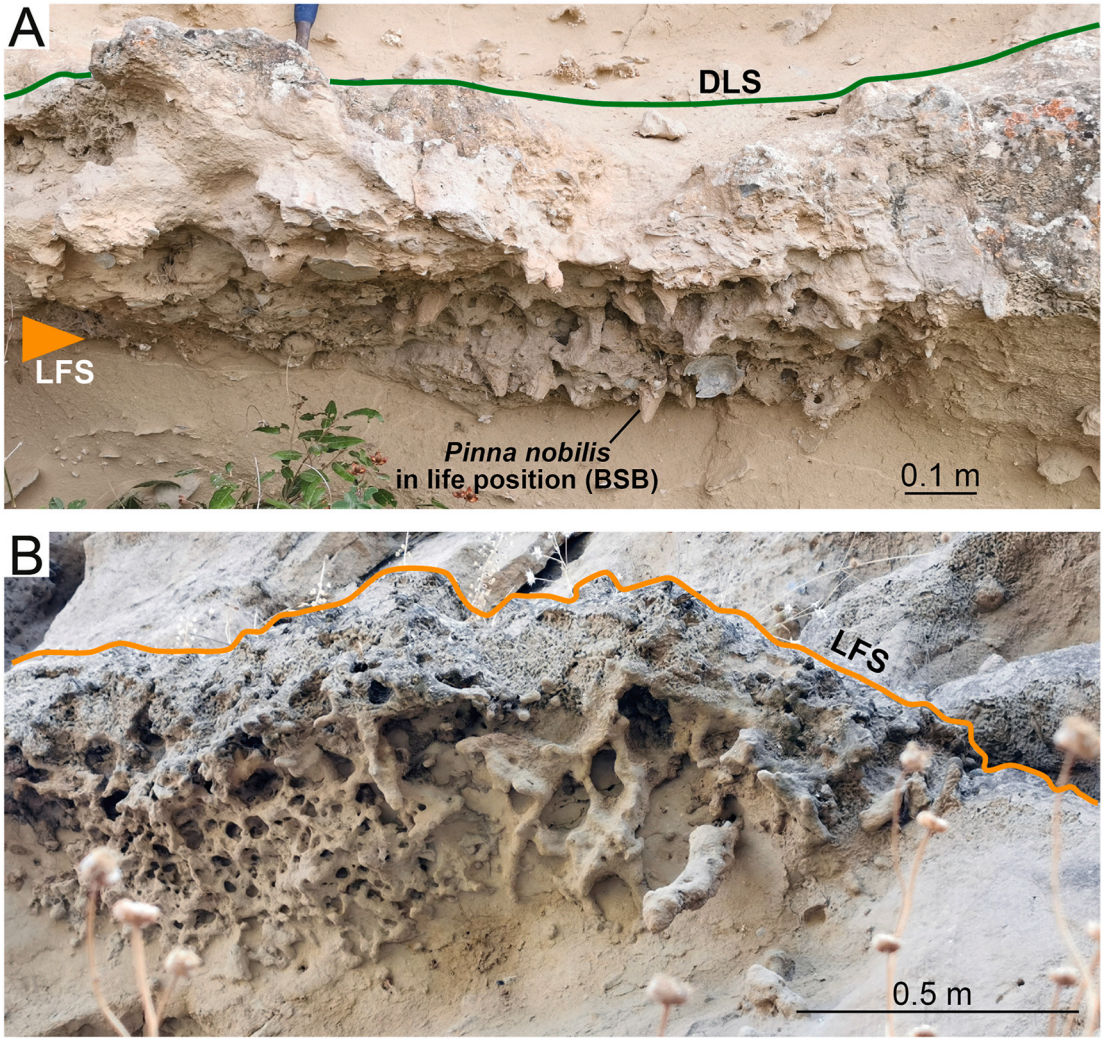

Fig. 4. (A) Example of burrowed condensed section in lower shoreface deposits (Zanclean of the Crotone Basin, southern Italy; modified from Zecchin et al., 2021), bounded below by a local flooding surface (LFS) penetrated by *Pinna nobilis* shells in life position (backlap shell bed, BSB), and by a downlap surface (DLS) above. (B) Example of local flooding surface marked by a well developed *Glossifungites* ichnofacies in lower shoreface deposits (Gelasian of the Crotone Basin, southern Italy; modified from Zecchin et al., 2022a).

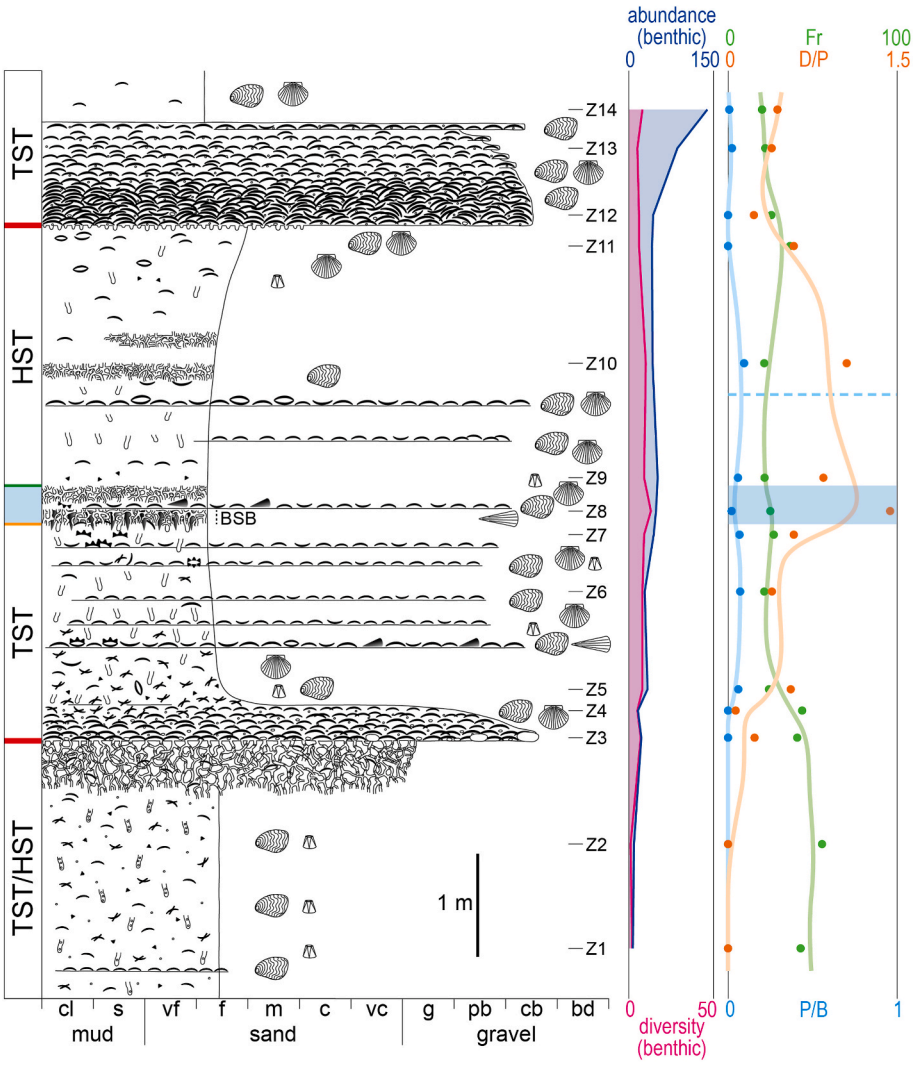

Fig. 5. Measured section showing a high-frequency sequence composed of shoreface deposits and bounded by wave-ravinement surfaces overlain by packed shell beds, in the Zanclean succession of the Crotone Basin, southern Italy (see Fig. 8 for symbols and abbreviations; modified from Zecchin et al., 2021). An uncertainty interval containing the maximum flooding surface is determined by integrating field data with parameters derived from the micropaleontological analysis, in particular the '% fragmentation' (Fr), the 'distal/proximal' (D/P), and in part the abundance and diversity. In particular, in this case the uncertainty interval coincides with the condensed section between the local flooding surface and the downlap surface, where the D/P and Fr curves show higher and lower values, respectively. The position of the maximum water depth surface corresponds to the peak od the plankton/benthos (P/B) curve, in the highstand systems tract.

Where sediment starvation on the shelf is pronounced, the CS may not accumulate and the LSF may coincide with the MFS, which therefore would assume physical expression (Zecchin and Catuneanu, 2013). On the contrary, if the sedimentation rate is high, such as in highly supplied shelves and/or in proximal settings, both LFSs and CSs may not develop and in such case there will be no surfaces with physical expression in the interval characterized by maximum flooding conditions (Zecchin and Catuneanu, 2013) (Fig. 7). In intermediate locations between proximal and distal settings, such as in the lower shoreface and shoreface-shelf transition zone, LFSs without clearly recognizable or with poorly developed BSBs were observed (Zecchin et al., 2021, 2022a) (Fig. 6). In such relatively proximal locations, LFSs and BSBs may be overlain by clastic sediments representing the youngest part of the transgressive sand sheet or healing-phase deposits, plus the older part of the prograding clastic wedge, and containing the cryptic MFS (Fig. 6).

The downlap surface (DLS; Kidwell, 1991) is a facies contact marking the top of the CS and the base of the highstand prograding clastic wedge in shelf settings (Figs. 1, 3 and 4A, 5 and 8). The DLS can be overlain by shell beds accumulated due to sediment starvation at the downward termination of the clinoforms (the 'downlap shell beds', DSB, Kidwell, 1991) (Fig. 1). The DLS and the MFS tend to diverge basinward on starved shelves characterized by the formation of CSs (Fig. 1); on the contrary, they may coincide in highly supplied shelves that do not experience sediment starvation (Zecchin and Catuneanu, 2013). The gradual transition between transgressive and highstand deposits in highly supplied shelves, which is not marked by any surface with physical expression, was called 'maximum flooding zone' (Siggerud and Steel, 1999; Cantalamessa and Di Celma, 2004; Di Celma and Cantalamessa, 2007). In proximal settings, within the shoreface, the DLS may be absent and the base of the clastic wedge does not coincide with any apparent surface (Zecchin et al., 2021, 2022a) (Figs. 1 and 7). The DLS is diachronous, becoming younger basinwards (Fig. 3).

In low-resolution studies, such as those based on seismic profiles, the MFS, LFS and DLS collapse to form a single surface downlapped by the highstand clinoforms (Fig. 2). This is the reason why early sequence stratigraphic studies considered the MFS and the DLS as the same surface.

The maximum water-depth surface (MWDS; Figs. 1, 3 and 5,6,7,8) was identified by Zecchin et al. (2021) on the basis of micropaleontological analyses, and is defined as a cryptic surface without sequence stratigraphic significance, marked by maximum values of the ratio between the number of planktonic and benthic foraminifera. The MWDS signifies the deepest water at syn-depositional time, which usually occurs above the MFS (Vecsei and Duringer, 2003; Catuneanu, 2006) (Fig. 1). In smaller, m-to decameter-scale sequences, the MWDS is commonly placed few cm to ca. 1 m above the MFS, in the early highstand systems tract, or at most, it may coincide with the MFS (Figs. 5–8). Water deepening in fact continues during the early highstand phase, until the progradation of the clastic wedge leads to a bathymetric decrease (Abbott, 1997; Carter et al., 1998; Catuneanu, 2006). The

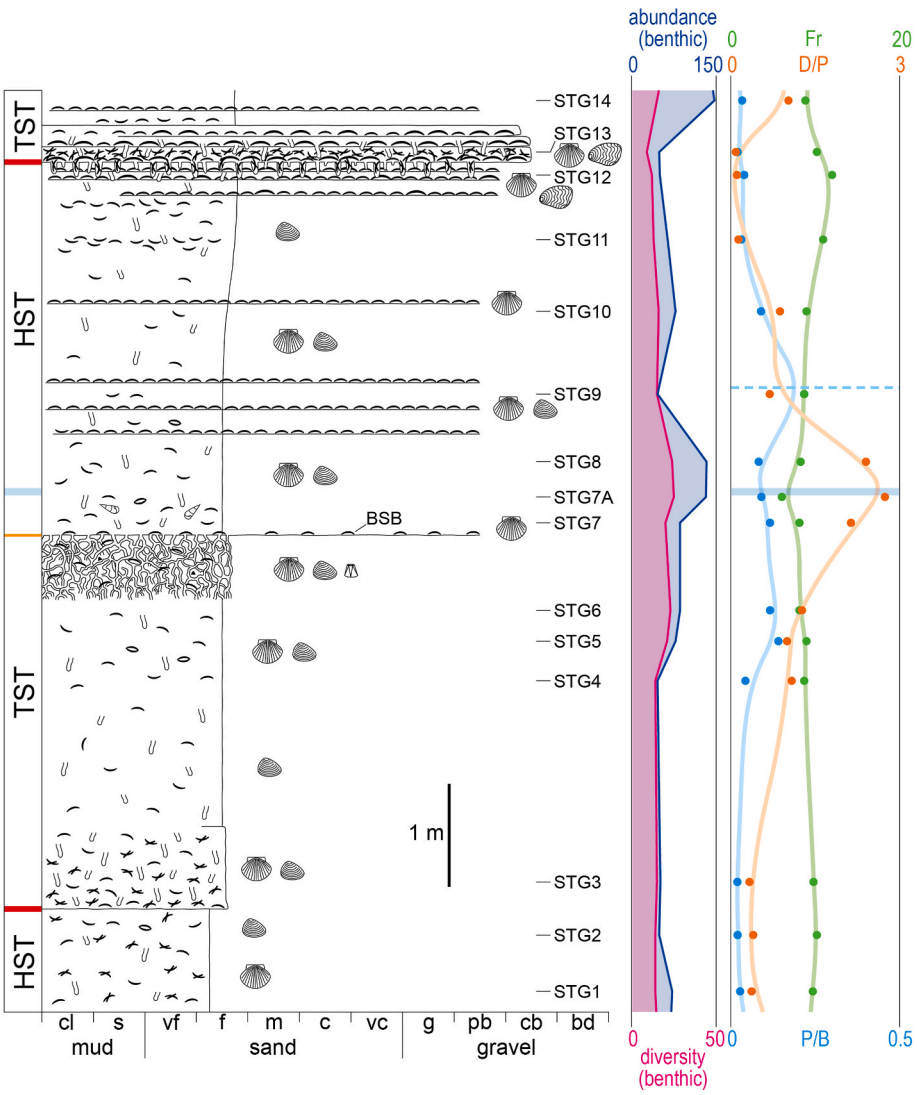

Fig. 6. Measured section showing a high-frequency sequence composed of shoreface deposits and bounded by wave-ravinement surfaces, in the Gelasian succession of the Crotone Basin, southern Italy (see Fig. 8 for symbols and abbreviations; modified from Zecchin et al., 2022a). In this example the uncertainty interval containing the maximum flooding surface is only based on micropaleontological analyses and is just few centimeters thick, from the minimum of the Fr curve and the maximum of the D/P curve. Also the abundance and diversity curves show higher values in this part of the sequence. The uncertainty interval lies some decimeters above the local flooding surface and does not exhibit physical features allowing its recognition in field.

MWDS is diachronous as it converges with the MFS towards the shoreline, but becomes younger basinward, diverging from the MFS (Catuneanu, 2006, 2022; Zecchin et al., 2021, 2022a) (Figs. 1, 3 and 9A). However, the MWDS and the MFS may also converge in increasingly starved conditions in the offshore direction (Fig. 9B), and they coincide if the sedimentation rate during highstand time overwhelms accommodation creation in any location along the shelf (Zecchin et al., 2022a) (Fig. 9C).

3. Methods for recognizing maximum flooding conditions in high-frequency sequences

3.1. Sedimentological criteria

Maximum flooding conditions are recorded within the most distal facies in a stratigraphic sequence, and some features are commonly considered as diagnostic to approximate the position of the MFS and/or to recognize the LFS and the DLS.

In particular, higher bioturbation levels in distal facies are commonly considered as diagnostic for maximum flooding conditions (Cantalamessa and Di Celma, 2004; Zecchin and Catuneanu, 2013). However, while this relationship may be valid to identify the interval, or part of it, representing relatively distal conditions in a stratigraphic sequence, the MFS not necessarily fall where the bioturbation level is the highest, as demonstrated by high resolution studies that considered an integrated approach to recognize stratigraphic surfaces (Zecchin et al., 2021, 2022a) (Fig. 7).

A well mappable surface featured by *Glossifungites* ichnofacies and locally overlain by shell concentrations, commonly develops in relatively distal deposits in stratigraphic sequences, and it typically corresponds to the LFS (plus the BSB) rather than the MFS (see Section 2) (Figs. 5 and 6). Since the LFS is the physical surface that documents the base of the CS and distal depositional settings in a sequence (Figs. 1, 3 and 4), its development usually precedes the timing of the MFS (Kidwell, 1991; Abbott and Carter, 1994; Zecchin and Catuneanu, 2013). LFSs must not be confused with non-depositional discontinuities bounding bedsets, which develop in the same depositional settings and are unrelated to shoreline shifts (Hampson, 2000; Zecchin et al., 2017). Its position within the maximum flooding interval, plus the commonly association with well-developed substrate-controlled ichnofacies and shell beds, aid to discriminate the LFS from bedset boundaries.

A sudden increase in grain size above the CS, marked by loosen shell beds, is commonly associated with the DLS, the end of accumulation of the CS and the onset of progradation of the highstand clastic wedge (Kidwell, 1991; Kondo et al., 1998; Zecchin and Catuneanu, 2013) (Figs. 1, 4A and 8). However, the DLS can disappear landwards, being replaced by a gradual coarsening upward trend in sandy shoreface deposits (Zecchin et al., 2021, 2022a) (Figs. 1 and 7). The DLS must not be

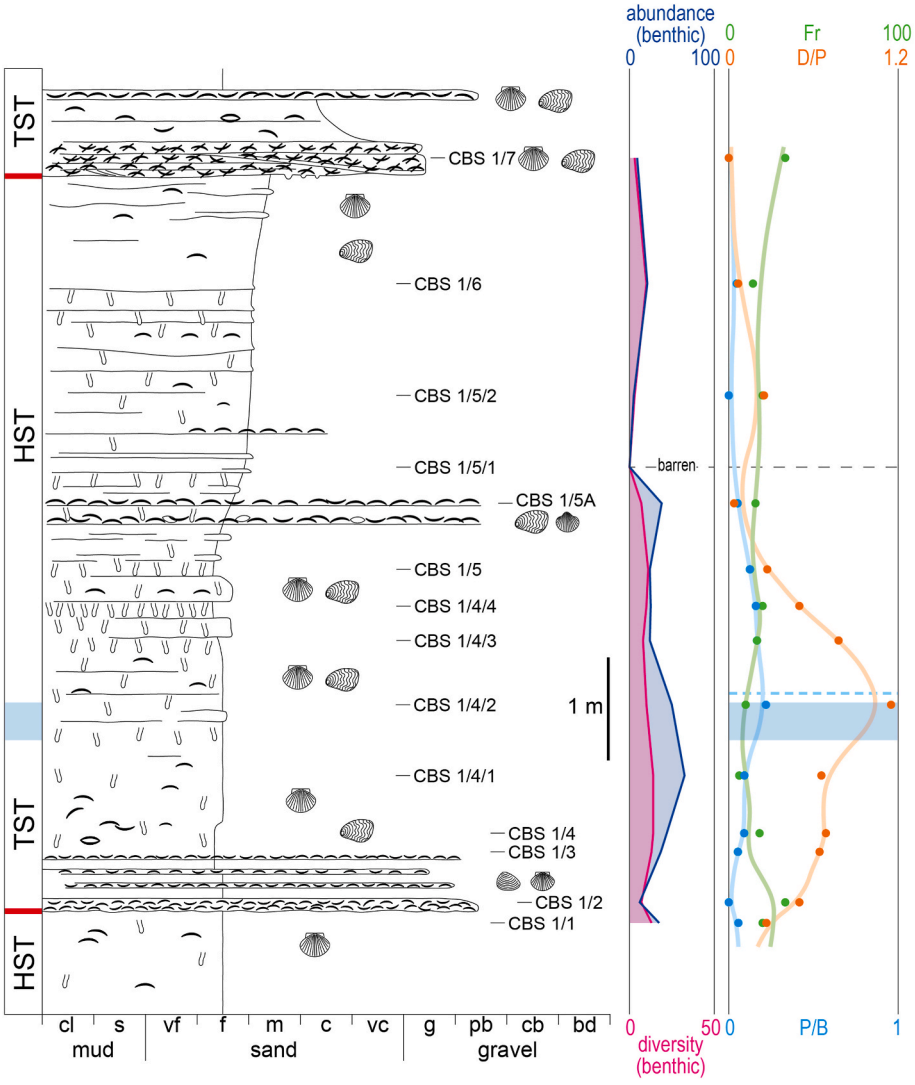

Fig. 7. Measured section showing a high-frequency sequence composed of shoreface deposits and bounded by wave-ravinement surfaces, in the Zanclean succession of the Crotone Basin, southern Italy (see Fig. 8 for symbols and abbreviations; modified from Zecchin et al., 2021). As in Fig. 6, in this case the uncertainty interval containing the maximum flooding surface is only based on micropaleontological analyses and is few decimeters thick, from the minimum of the Fr curve and the maximum of the D/P curve. It sists in sands without physical diagnostic features, ca. 1 m below the interval characterized by maximum bioturbation.

confused with erosional discontinuities bounding bedsets, which are also associated with an abrupt increase in grain size (Hampson, 2000; Zecchin et al., 2017). The position of the DLS just above the CS allows it to be discriminated from bedset boundaries.

Field and core data are therefore essential to precisely recognize LFSs and DLSs but only to approximate the position of MFSs, which should be determined more precisely by means of the integration of several other criteria.

3.2. Diagenetic criteria

Sediment starvation in shelf settings during transgressive phases and maximum flooding conditions may favor diagenetic processes mainly associated with LFSs and in general with the formation of CSs (Fig. 10). In particular, sediment starvation during the formation of the LFS favors ionic diffusion below that surface and extensive carbonate cementation (Taylor et al., 1995; Morad et al., 2000, 2013; Ketzer et al., 2003). The cementation is also favored by the availability of carbonate-rich skeletal material in BSBs (Fig. 4A), as well as by the presence of substrate-controlled ichnofacies and organic matter just below the LFS (Taylor et al., 2000; Zecchin and Caffau, 2012) (Fig. 4B). The increased bioturbation commonly found in sediments associated with maximum flooding conditions also favors diffuse cementation. Typical precipitates in conditions of reduced sedimentation rate during the accumulation of the CS include autochthonous glaucony (Amorosi, 1995, Fig. 10), siderite and other carbonates forming hardgrounds.

Diagenetic criteria represent therefore additional evidence aiding to recognize the interval characterized by maximum flooding conditions within stratigraphic sequences and facies contacts documenting sediment starvation, in particular the LFS. However, these criteria alone do not provide elements to pick the MFS more precisely with respect to the sedimentological evidence.

3.3. Micropaleontological criteria

3.3.1. Abundance and diversity

The abundance (total count) and diversity (sum of species) of microfossils or nannofossils for each sample were already used for approximating the position of the MFS in sequences (Figs. 5–8), as a higher number of individuals as well as of species are generally inferred to reflect deeper bathymetric conditions and lower sedimentation rates (e.g., Loutit et al., 1988; Fillon, 2007; Gutiérrez Paredes et al., 2017).

Not only water depth changes, but also local productivity, dilution by terrigenous sediments and dissolution (Fillon, 2007), as well as oxygenation, can affect these two parameters, and this is the reason why, although both abundance and diversity tend to increase toward maximum flooding conditions and deeper settings, their peaks can be multiple and not always coinciding with more univocal maxima and

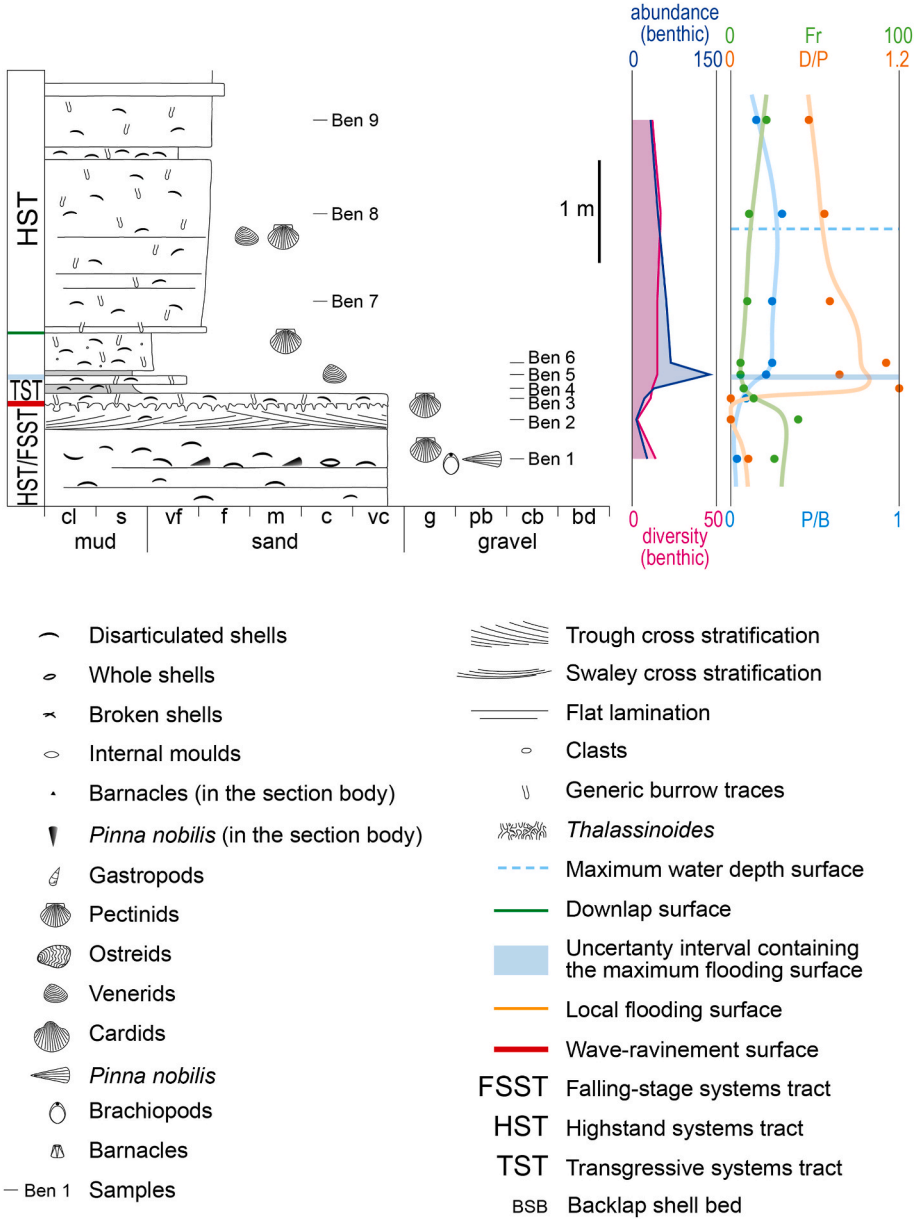

Fig. 8. Measured section showing a high-frequency sequence composed of shoreface and shoreface-shelf transition deposits and bounded below by a wave-ravinement surface, in the Gelasian succession of the Crotone Basin, southern Italy (modified from Zecchin et al., 2021). The uncertainty interval containing the maximum flooding surface is based on micropaleontological analyses and is few centimeters thick, from the minimum of the Fr curve and the maximum of the D/P curve. Also the abundance of curve exhibits a peak in that interval.

minima of other parameters such as the percentage of fragmentation and the distal/proximal (see next Sections) (Zecchin et al., 2021, 2022a) (Figs. 5–8). It is therefore suggested to consider with caution the abundance and diversity peaks and to compare them with the results deriving from other methods.

3.3.2. *Percentage of fragmentation (Fr)*

The '% fragmentation' parameter (Fr; Figs. 5–8) was introduced by Zecchin et al. (2021) and considers naturally fragmented benthic foraminifera specimens for each sample. The Fr parameter is calculated as follows:

Fr = (number of fragmented specimens of benthic foraminifera/total number of specimens of benthic foraminifera) x 100.

The evaluation of this parameter requires criteria consistency. Just as an example, if specimens with less than a given percentage of preservation are considered as fragmented, this must be valid for all samples.

It is expected that the Fr parameter is a proxy for energy, and therefore it should reflect changes of wave and/or current strength, as well as shoreline shifts and water depth variations associated with relative sea-level and/or sediment supply changes (Zecchin et al., 2021, 2022a). In high-frequency sequences, lower values of the Fr parameter are therefore expected to be associated with distal deposits, corresponding to maximum flooding conditions (e.g., Zecchin et al., 2021, 2022a) (Figs. 5–8).

The Fr parameter usually works well in most cases, from sequences documenting large environmental changes to those associated with very limited shoreline shifts and facies changes (Zecchin et al., 2021, 2022a).

3.3.3. *Distal/proximal parameter (D/P)*

The 'distal/proximal' parameter (D/P; Figs. 5–8) was introduced by Zecchin et al. (2021) and is defined as the ratio between relatively distal on relatively proximal species of benthic foraminifera for each sample. The D/P parameter is calculated as follows:

D/P = percentage sum of relatively distal benthic foraminifera/percentage sum of relatively proximal benthic foraminifera.

Due to the way the D/P parameter is defined, the species of relatively distal and proximal benthic foraminifera may vary case by case, in relation of the taxa present in a given succession as well as of the

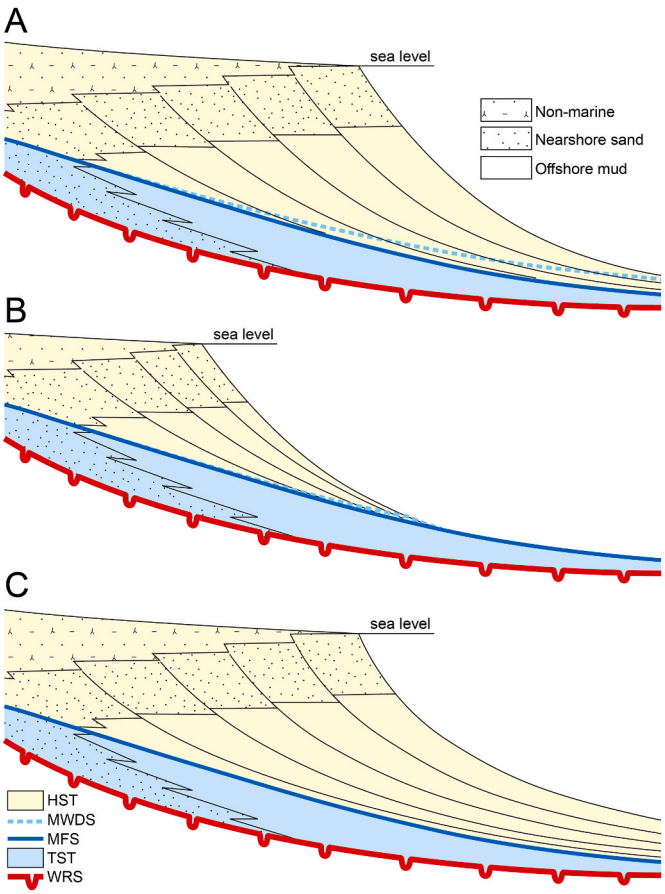

Fig. 9. Variability of the offset between the maximum flooding surface and the maximum water depth surface (from Zecchin et al., 2022a). (A) In most cases the offset between the two surfaces increases offshore during highstand time, as the increasing bathymetry linked to relative sea-level rise is countered later by the progradation of the clastic wedge seaward. (B) Increasingly starved conditions in distal locations during highstand time lead to a convergence between the maximum flooding and maximum water depth surfaces. (C) If the sedimentation rate exceeds accommodation creation in any location during highstand time, a bathymetric increase does not occur and the maximum flooding and maximum water depth surfaces coincide. Abbreviations: HST – highstand systems tract; MFS – maximum flooding surface; MWDS – maximum water depth surface; TST – transgressive systems tract; WRS – wave-ravinement surface.

position of a given section along depositional dip. For example, the proximal and distal species to be considered for a succession ranging from outer shelf to shoreface-shelf transition deposits are not the same for another made up of shoreface-shelf transition and shoreface deposits, and therefore the proximal forms considered for a succession may also become the distal ones for another succession representing a different transect along depositional dip. A certain degree of variability in the results may derive from the choice of which species to consider in the count among those distal and proximal, and this may be in part at the discretion of the micropaleontologist but must be consistent for all samples.

The D/P parameter is expected to be a proxy for shoreline shifts, as benthic foraminifera are sensitive to decreasing and increasing sedimentation rates at a given location along depositional dip, associated respectively with transgressions and regressions (Zecchin et al., 2021, 2022a). It is expected that the curve of the D/P parameter responds immediately to increasing sedimentation rates at the onset of the highstand normal regression, as relatively distal species, which prefer sediment-starved settings, usually decrease suddenly in these conditions.

Higher values of the D/P parameter are therefore expected to indicate more distal settings (Figs. 5–8). Maxima of the D/P parameter and minima of the Fr parameter are usually close (from few cm to ca. 1 m) in high-frequency sequences, and this allows to define a relatively thin uncertainty interval, within which the cryptic MFS should lie (Zecchin et al., 2021, 2022a) (Figs. 5–8).

The D/P parameter works well in shallow marine high-frequency sequences, mimicking both transgressive and regressive trends and showing a prominent peak close to the MFS. While this parameter provides the best results in case of high-frequency sequences that document significant environmental changes, or in those sequences associated with limited shoreline shift and dominated by lower shoreface deposits (Figs. 5–8), it tends to become ineffective if limited shoreline shifts are associated with only very proximal (e.g., middle to upper shoreface) deposits (Zecchin et al., 2021, 2022a). Limitations in the effectiveness of the parameter were also observed in successions representing relatively short transects along the shelf, which does not include a variety of benthic foraminifera with really differentiated distal and proximal taxa (Zecchin et al., 2022a).

3.3.4. *Plankton/benthos parameter (P/B)*

The 'plankton/benthos' parameter (P/B; Figs. 5–8) is well known in micropaleontological studies and is defined as the ratio between planktonic and benthic foraminifera, which is calculated as follows:

P/B = total number of planktonic foraminifera/total number of benthic foraminifera.

Since it considers the planktonic foraminifera, the P/B parameter is sensitive to the water mass rather than the substrate, and therefore it is inferred to be a proxy for water depth changes rather than transgressive-regressive trends. The peak of the P/B parameter is inferred to be associated with the MWDS, which usually lies up to ca. 1 m above the MFS in high-frequency sequences (see Section 2; Zecchin et al., 2021, 2022a) (Figs. 5–8).

The evidence that planktonic foraminifera tend to become scarce landwards explains why the P/B parameter is usually ineffective in middle to upper shoreface deposits (Zecchin et al., 2021).

3.3.5. *Statistical analyses*

Paleobathymetric changes as well as the position of the MFS within sequences were also evaluated on the basis of statistical analyses of benthic foraminifera associations (Naish and Kamp, 1997b). These studies were performed in the late Pliocene sequences of New Zealand, where the foraminifera associations, determined by cluster analysis, have been compared to the distribution of benthic foraminifera along the modern shelf (Naish and Kamp, 1997b). Such approach allows to recognize a relatively large interval of maximum water deepening that should also contain the cryptic MFS, spanning the top of the transgressive systems tract and the lower part of the highstand systems tract, and therefore this is a relatively low-resolution method.

3.4. *Geophysical criteria*

Information from well logs, such as gamma ray, resistivity and spontaneous potential (SP) logs, was used to infer the position of the MFS, or more in general of the CS, in stratigraphic sequences (Loutit et al., 1988; Posamentier and Allen, 1999; Catuneanu, 2022, Fig. 11). In particular, gamma ray counts tend to increase in deeper water, organic- and/or glauconite-rich muds recording sediment starvation, which are usually associated with higher amounts of uranium and potassium (Loutit et al., 1988). In marine sequences, deep-water muds recording maximum flooding conditions are associated with positive values of SP logs and lower values of resistivity logs.

In cores, a good correspondence between finer, distal facies and higher values of the gamma ray was generally observed (Posamentier and Allen, 1999; Naish et al., 2005) (Fig. 11). However, care must be used to infer maximum flooding conditions from gamma ray and other

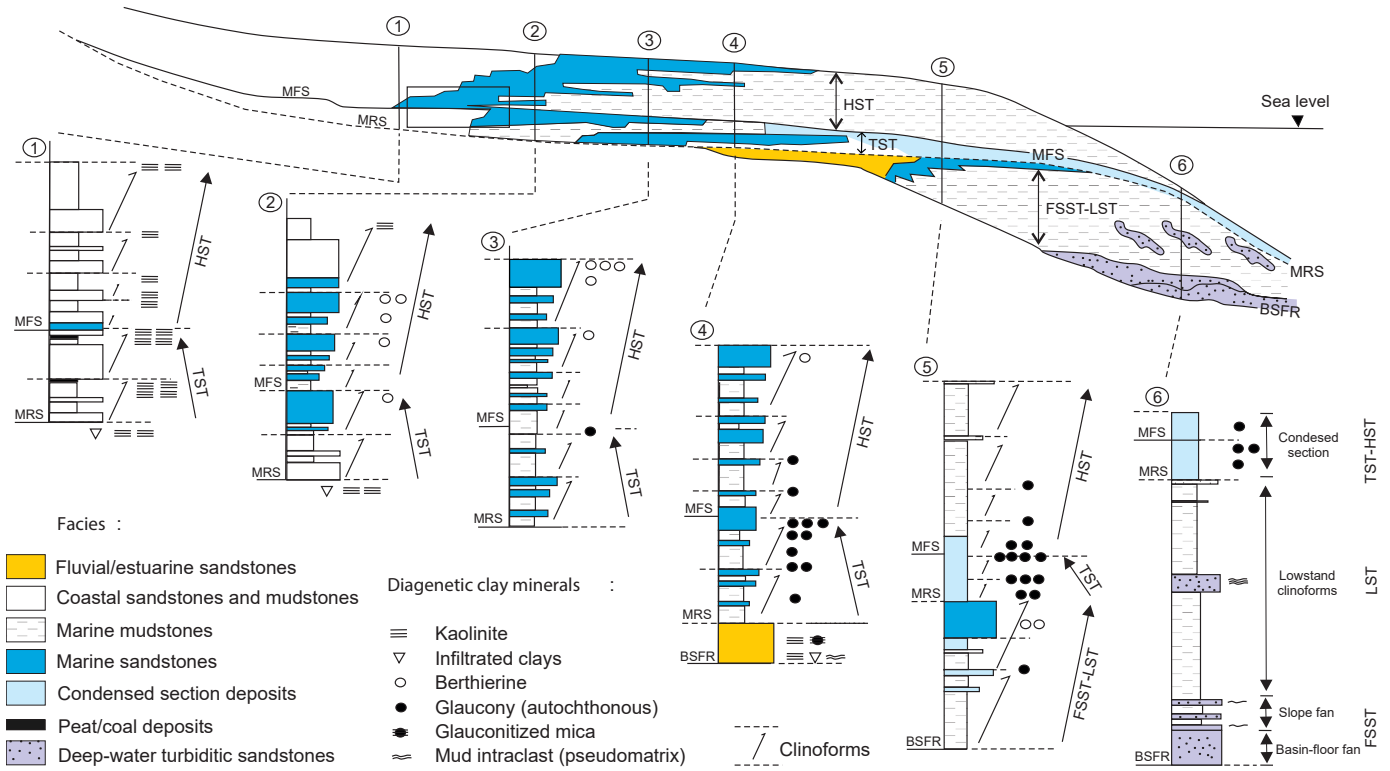

Fig. 10. Distribution of diagenetic clay minerals in a sequence stratigraphic framework (modified from Ketzer et al., 2003). Abbreviations: MFS – maximum flooding surface; MRS – maximum regressive surface; BSFR – basal surface of forced regression; HST – highstand systems tract; TST – transgressive systems tract; LST – lowstand systems tract; FSST – falling-stage systems tract.

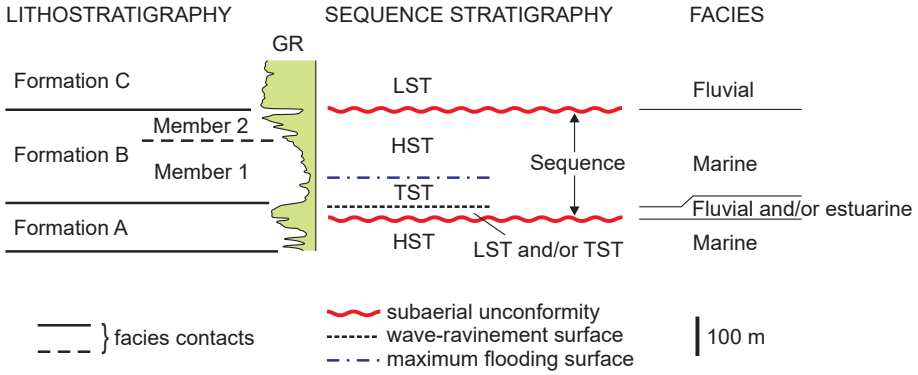

Fig. 11. Lithostratigraphy and sequence stratigraphy of a facies succession (modified from Posamentier and Allen, 1999). The position of the maximum flooding surface is approximated by the peak of the gamma ray log. GR – gamma-ray log; LST – lowstand systems tract; TST – transgressive systems tract; HST – highstand systems tract.

logs, as also organic-rich clays accumulated in different positions within a sequence can give similar results (Posamentier and Allen, 1999). Also, high gamma ray counts were also found in heavy mineral-bearing layers in upper shoreface and foreshore deposits unrelated to maximum flooding conditions (Hampson et al., 2008). Moreover, diagenetic processes in CSs may lead to variable responses of well logs, resulting in false or imprecise responses. For a reliable determination of the position of the MFS, integration with other methods is therefore required.

3.5. Geochemical criteria

Both organic and inorganic geochemistry can provide clues to identify surfaces or intervals associated with maximum flooding conditions, particularly within mud-dominated successions (e.g., Harris et al., 2013, 2018; Playter et al., 2018; LaGrange et al., 2020; Catuneanu, 2022). The amount of total organic carbon (TOC) in fine-grained successions depends on several parameters, including organic productivity, preservation potential, and terrigenous sediment supply (Dong et al., 2018). Despite this complexity, the analysis of TOC distribution is somewhat simplified because all three main parameters (i.e., productivity, preservation, and sediment supply) are linked to changes in relative sea level at syn-depositional time (Fleck et al., 2002; Arthur and Sageman, 2005; Bohacs et al., 2005; Dong et al., 2018; Harris et al., 2018). Stages of transgression during relative sea-level rise promote influxes of nutrient-rich upwelled water, which increase surface-water productivity; enhance water-column stratification, leading to the development of bottom-water anoxia; and result in the trapping of terrigenous sediment in coastal and nearshore environments, favoring the development of organic-rich condensed sections offshore (Dong et al., 2018; Harris et al., 2018) (Fig. 12).

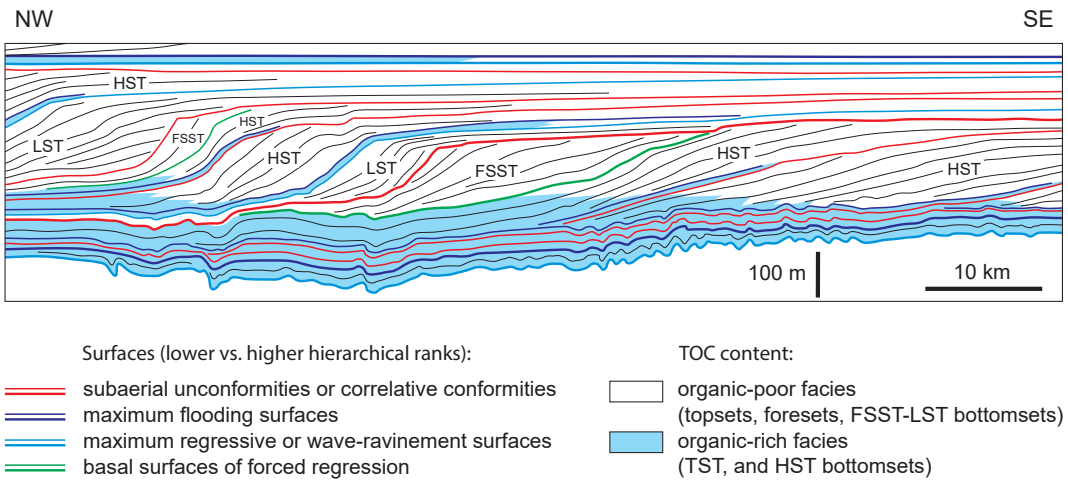

Fig. 12. Distribution of total organic carbon (TOC) within a sequence stratigraphic framework, based on seismic acoustic impedance data calibrated with well data (Quintuco-Vaca Muerta system, Tithonian-Lower Valanginian, Neuquén Basin, Argentina; modified from Dominguez et al., 2016, 2020; Reijenstein et al., 2020). Highest TOC amounts characterize transgressive systems tracts and the bottomsets of highstand systems tracts and straddle the maximum flooding surface. Abbreviations: FSST – falling-stage systems tract; LST – lowstand systems tract; TST – transgressive systems tract; HST – highstand systems tract.

Studies of the proxies for restriction of water masses (Mo/TOC), redox conditions (Mo/Al and S/Fe) and productivity of biogenic silica converge to the conclusion that TOC values are typically highest at or around maximum flooding surfaces (Harris et al., 2018). In lower resolution studies, the intervals of higher TOC values typically straddle the maximum flooding surface, encompassing the transgressive condensed sections and the bottomsets of the overlying highstand systems tracts (Fig. 12). However, higher resolution geochemical data coupled with sedimentological data from core document that the highest TOC values may in fact be recorded just above the maximum flooding surface within a studied section (Harris et al., 2018), as the horizon which corresponds to the deepest water at syn-depositional time is often above the maximum flooding surface at any location (Catuneanu, 2006, 2022; Zecchin et al., 2021, Figs. 5–8). It is therefore likely that the organic geochemistry criteria linked to the TOC concentrations in the sedimentary record may in fact pinpoint to MWDS rather than MFS surfaces.

Inorganic geochemistry proxies are based on major, minor and trace elements, which can also be linked to changes in relative sea level (Harris et al., 2013, 2018; Dong et al., 2018; Playter et al., 2018; LaGrange et al., 2020). For example, the influx of clay into sedimentary basins, as measured by the Zr/La ratio, was shown to increase during relative sea-level rise and particularly during transgression (Playter et al., 2018). Documentation of trace element renewal (e.g., Mo) in partially restricted basins can also be related to the relative sea level, as communication between the restricted basin and the open ocean increases during stages of relative sea-level rise and transgression (Harris et al., 2013; Turner et al., 2016). Among the elemental proxies that are most relevant to sequence stratigraphy, lows in terrigenous proxies (Ti/Al), minima in grain size proxies (Si/Al, Zr/Al, Zr/Nb, Zr/Rb, Y/Al, Y/Rb), and the increase in proxies for biogenic silica (Si/Al) are found to be closely associated with maximum flooding surfaces (Ratcliffe et al., 2012; Sano et al., 2013; Turner et al., 2016; Harris et al., 2018).

Notwithstanding the geochemical trends reported in these studies, the composition of the terrigenous sediment that reaches a sedimentary basin during cycles of relative sea-level change also depends on the types of rocks that are subject to weathering and erosion in the provenance areas. Such considerations also need to be taken into account when interpreting geochemical data for sequence stratigraphic purposes, in order to select the geochemical proxies that are most pertinent under the specific circumstances of any particular case study.

4. Discussion and conclusions

Several independent criteria allow to recognize characteristic surfaces associated with maximum flooding conditions in high-frequency sequences, although the effectiveness of these criteria in accurately picking the MFS and/or facies contacts varies considerably. While all methods are sufficient to roughly recognize the maximum flooding interval, the analysis of sedimentary facies and diagenetic features is the most effective to identify the LFS and the DLS, as they have physical appearance and, in the case of the LFS, marked diagenetic signature (Figs. 4–8). In contrast, micropaleontological, geophysical and geochemical criteria are more useful to approximate the position of the MFS and the MWDS, although the resolution at which this can be achieved varies significantly. In particular, micropaleontological criteria, and specifically the use of the Fr and D/P parameters, allow to reveal relatively thin intervals containing the cryptic MFS, as well as the position of the MWDS (P/B parameter) (Zecchin et al., 2021, 2022a) (Figs. 5–8), and therefore they are to be considered as effective tools for high-resolution studies. Also, organic geochemical criteria (TOC) have proven to be useful in high-resolution studies for the identification of the MWDS (Harris et al., 2018), and for this reason a specific comparison of this method with the results from the P/B parameter would deserve further study.

As stated in Section 3.4, the employment of geophysical criteria needs to be accompanied by other datasets, such as micropaleontological and petrographic, for reliable results. For example, high gamma-ray values often signify organic-rich shales associated with maximum flooding conditions (Fig. 12), but sandstones derived from a granitic provenance can also display a high-gamma log response due to the presence of minerals with radioactive elements. Therefore, the interpretation of geophysical well logs requires calibration with rock data collected from core or rock cuttings, to ensure reliable results. Seismic data also require calibration with higher resolution data from wells to separate stratigraphic surfaces, such as the LFS, MFS and DLS (Fig. 1), which often tune into single seismic reflections (Fig. 2).

An integration with other methods is also recommended for the use of both organic and inorganic geochemical data to identify surfaces associated with the maximum flooding interval in high-frequency sequences. Challenges in identifying stratigraphic cyclicity in lithologically monotonous mudstone successions make the integration of geochemical data with conventional facies analyses increasingly common (LaGrange et al., 2020). The correct interpretation of elemental proxies requires elemental data to be calibrated with mineralogical data,

to ensure the proper usage of the former for the purposes of sequence stratigraphy (e.g., to discern between the depositional and diagenetic trends recorded by elemental data; LaGrange et al., 2020). The position of maximum flooding surfaces is also best constrained where geochemical proxies are calibrated with biostratigraphic data (e.g., the highest abundance of microfossils, the highest value of the D/P parameter and the lowest value of the Fr parameter within a condensed section; Gutiérrez Paredes et al., 2017; Zecchin et al., 2021, 2022a), as well as seismic data (e.g., tracing downlap surfaces into the depocenters).

Overall, the most effective approach for the recognition of surfaces related to the maximum flooding interval in high-resolution studies seems to be the integration between field/core data and the micropaleontological parameters described above. The possibility of constraining the MFS within an uncertainty interval between the negative peak of the Fr parameter and the positive peak of the D/P parameter (Zecchin et al., 2021, 2022a) (Figs. 5–8) represents a step forward in high-resolution sequence stratigraphic analyses, implicitly confirming the common cryptic nature of that surface. The closeness of these peaks observed in most sequences is an indication that the Fr and D/P parameters, which are calculated independently, do not record simply local energy variations but true shoreline shifts linked to relative sea-level and/or sediment supply changes. The fact that the Fr and D/P parameters are ratios, rather than sums as in the case of the 'abundance' and 'diversity' of microfossils, makes them more independent of environmental variables, and hence more reliable for stratigraphic studies.

Looking forward, the integration between micropaleontological and geochemical methods merits to be tested more in detail, as this approach may potentially contribute to further refine the positioning of the MFS and, in more general terms, of other cryptic sequence stratigraphic surfaces (such as the basal surface of forced regression and the correlative conformity) within stratigraphic sequences.

Declaration of competing interest

The authors declare that they have no known competing financial interests or personal relationships that could have appeared to influence the work reported in this paper.

Data availability

The data that has been used is confidential.

Acknowledgments

We thank Claudio Di Celma, Thomas Hadlari, Angelos G. Maravelis and the Editor Istvan Csato for helpful and constructive comments during the review process.

References

Abbott, S.T., Carter, R.M., 1994. The sequence architecture of Mid-Pleistocene (c.1.1.–0.4Ma) cyclothems from New Zealand: facies development during a Period of orbital control on sea-level cyclicity. In: De Boer, P.L., Smith, D.G. (Eds.), Orbital Forcing and Cyclic Sequences, vol. 19. IAS Special Publication, pp. 367–394.

Abbott, S.T., 1997. Foraminiferal paleobathymetry and mid-cycle architecture of mid-Pleistocene depositional sequences, Wanganui Basin, New Zealand. Palaios 12, 267–281.

Amorosi, A., 1995. Glaucony and sequence stratigraphy: conceptual framework of distribution in siliciclastic sequences. J. Sediment. Res. B65, 419–425.

Arthur, M.A., Sageman, B.B., 2005. Sea-Level control on source-rock development: perspectives from the holocene black Sea, the mid-cretaceous western interior basin of north America, and the late devonian appalachian basin. In: Harris, N.B. (Ed.), The Deposition of Organic-Carbon-Rich Sediments: Models, Mechanisms, and Consequences, vol. 82. SEPM Special Publication, pp. 35–59.

Baum, G.R., Vail, P.R., 1988. Sequence stratigraphic concepts applied to Paleogene outcrops, Gulf and Atlantic basins. In: Wilgus, C.K., Hastings, B.S., Kendall, C.G.StC., Posamentier, H.W., Ross, C.A., Van Wagoner, J.C. (Eds.), Sea Level Changes: an Integrated Approach, vol. 42. SEPM Special Publication, pp. 39–45.

Bohacs, K.M., Grabowski, G.J., Carroll, A.R., Mankiewicz, P.J., Gerhardt, K.J., Schwalbach, J.R., Wegner, M.B., Simo, J.A., 2005. Production, destruction, and dilution – the many paths to source rock development. In: Harris, N.B. (Ed.), The Deposition of Organic-Carbon-Rich Sediments: Models, Mechanisms, and Consequences, vol. 82. SEPM Special Publication, pp. 61–101.

Brown Jr., L.F., Benson, J.M., Brink, G.J., Doherty, S., Jollands, A., Jungslager, E.H.A., Keenan, J.H.G., Muntingh, A., van Wyk, N.J.S., 1995. Sequence Stratigraphy in Offshore South African Divergent Basins: an Atlas on Exploration for Cretaceous Lowstand Traps by Soekor (Pty) Ltd. AAPG Studies in Geology, Tulsa, Oklahoma, p. 184. #41.

Cantalamessa, G., Di Celma, C., 2004. Sequence response to syndepositional regional uplift: insights from high-resolution sequence stratigraphy of late Early Pleistocene strata, Periadriatic Basin. Central Italy. Sediment. Geol. 164, 283–309.

Carter, R.M., Fulthorpe, C.S., Naish, T.R., 1998. Sequence concepts at seismic and outcrop scale: the distinction between physical and conceptual stratigraphic surfaces. Sediment. Geol. 122, 165–179.

Catuneanu, O., 2006. Principles of Sequence Stratigraphy. Elsevier, Amsterdam, p. 386.

Catuneanu, O., 2022. Principles of Sequence Stratigraphy, second ed. Elsevier, Amsterdam, p. 494.

Catuneanu, O., Zecchin, M., 2013. High-resolution sequence stratigraphy of clastic shelves II: controls on sequence development. Mar. Petrol. Geol. 39, 26–38.

Di Celma, C., Ragaini, L., Cantalamessa, G., Landini, W., 2005. Basin physiography and tectonic influence on the sequence architecture and stacking pattern: pleistocene succession of the Canoa Basin (central Ecuador). GSA Bull. 117, 1226–1241.

Di Celma, C., Cantalamessa, G., 2007. Sedimentology and high-frequency sequence stratigraphy of a forearc extensional basin: the Miocene Caleta Herradura Formation, Mejillones Peninsula, northern Chile. Sediment. Geol. 198, 29–52.

Dominguez, R.F., Continanzia, M.J., Mykietiuk, K., Ponce, C., Pérez, G., Guerello, R., Lanusse Noguera, I., Caneva, M., Di Benedetto, M., Catuneanu, O., Cristallini, E., 2016. Organic-rich stratigraphic units in the vaca Muerta formation, and their distribution and characterization in the Neuquén Basin (Argentina). In: Unconventional Resources Technology Conference. URTeC, pp. 1–12. https://doi.org/10.15530/urtec-2016-2456851, 2016.

Dominguez, R.F., Catuneanu, O., Reijenstein, H., Notta, R., Posamentier, H.W., 2020. Sequence stratigraphy and the three-dimensional distribution of organic-rich units. In: Minisini, D., Fantin, M., Lanusse Noguera, I., Leanza, H.A. (Eds.), Integrated Geology of Unconventionals: the Case of the Vaca Muerta Play, vol. 121. AAPG Memoir, Argentina, pp. 163–200.

Dong, T., Harris, N.B., Ayranci, K., 2018. Relative sea-level cycles and organic matter accumulation in shales of the Middle and Upper Devonian Horn River Group, northeastern British Columbia, Canada: insights into sediment flux, redox conditions, and bioproductivity. GSA Bull. 130, 859–880.

Fillon, R.H., 2007. Biostratigraphy and condensed sections in deepwater settings. In: Weimer, P., Slatt, R. (Eds.), Introduction to the Petroleum Geology of Deepwater Settings, AAPG Studies in Geology 57 AAPG/Datapages Discovery Series 8.

Fleck, S., Michels, R., Ferry, S., Malartre, F., Elion, P., Landais, P., 2002. Organic geochemistry in a sequence stratigraphic framework: the siliciclastic shelf environment of Cretaceous series, SE France. Org. Geochem. 33, 1533–1557.

Galloway, W.E., 1989. Genetic stratigraphic sequences in basin analysis I: architecture and genesis of flooding-surface bounded depositional units. AAPG (Am. Assoc. Pet. Geol.) Bull. 73, 125–142.

Gutiérrez Paredes, H.C., Catuneanu, O., Romano, U.H., 2017. Sequence stratigraphy of the Miocene section, southern Gulf of Mexico. Mar. Petrol. Geol. 86, 711–732.

Hampson, G.J., 2000. Discontinuity surfaces, clinoforms, and facies architecture in a wave-dominated, shoreface-shelf parasequence. J. Sediment. Res. 70, 325–340.

Hampson, G.J., Rodriguez, A.B., Storms, J.E.A., Johnson, H.D., Meyer, C.T., 2008. Geomorphology and high-resolution stratigraphy of progradational wave-dominated shoreline deposits: impact on reservoir-scale facies architecture. In: Hampson, G.J., Steel, R.J., Burgess, P.M., Dalrymple, R.W. (Eds.), Recent Advances in Models of Siliciclastic Shallow-Marine Stratigraphy, vol. 90. SEPM Special Publication, pp. 117–142.

Harris, N.B., Mnich, C.A., Selby, D., Korn, D., 2013. Minor and trace element and Re-Os chemistry of the Upper Devonian Woodford Shale, Permian Basin, West Texas: insights into metal abundance and basin processes. Chem. Geol. 356, 76–93.

Harris, N.B., McMillan, J.M., Knapp, L.V., Mastalerz, M., 2018. Organic matter accumulation in the upper devonian duvernay formation, western Canada sedimentary basin, from sequence stratigraphic analysis and geochemical proxies. Sediment. Geol. 376, 185–203.

Ketzer, J.M., Morad, S., Amorosi, A., 2003. Predictive diagenetic clay-mineral distribution in siliciclastic rocks within a sequence stratigraphic framework. In: Worden, R.H., Morad, S. (Eds.), Clay Mineral Cements in Sandstones, vol. 34. IAS Special Publication, pp. 43–61.

Kidwell, S.M., 1991. Condensed deposits in siliciclastic sequences: expected and observed features. In: Einsele, G., Ricken, W., Seilacher, A. (Eds.), Cycles and Events in Stratigraphy. Springer-Verlag, Berlin, pp. 682–695.

Kondo, Y., Abbott, S.T., Kitamura, A., Kamp, P.J.J., Naish, T.R., Kamataki, T., Saul, G.S., 1998. The relationship between shell bed type and sequence architecture: examples from Japan and New Zealand. Sediment. Geol. 122, 109–127.

LaGrange, M.T., Konhauser, K.O., Catuneanu, O., Harris, B.S., Playter, T.L., Gingras, M. K., 2020. Sequence stratigraphy in organic-rich marine mudstone successions using chemostratigraphic datasets. Earth Sci. Rev. 203, 103137.

Loutit, T.S., Hardenbol, J., Vail, P.R., Baum, G.R., 1988. Condensed sections: the key to age determination and correlation of continental margin sequences. In: Wilgus, C.K., Hastings, B.S., Kendall, C.G.StC., Posamentier, H.W., Ross, C.A., Van Wagoner, J.C. (Eds.), Sea Level Changes: an Integrated Approach, vol. 42. SEPM Special Publication, pp. 183–213.

Maravelis, A.G., Catuneanu, O., Nordsvan, A., Landenberger, B., Zelilidis, A., 2018. Interplay of tectonism and eustasy during the early permian icehouse: southern sydney basin, southeast Australia. Geol. J. 53, 1372–1403.
Morad, S., Ketzer, J.M., De Ros, L.F., 2000. Spatial and temporal distribution of diagenetic alterations in siliciclastic rocks: implications for mass transfer in sedimentary basins. Sedimentology 47, 95–120.
Morad, S., Ketzer, J.M., De Ros, L.F., 2013. Linking diagenesis to sequence stratigraphy: an integrated tool for understanding and predicting reservoir quality distribution. In: Morad, S., Ketzer, J.M., De Ros, L.F. (Eds.), Linking Diagenesis to Sequence Stratigraphy, vol. 45. IAS Special Publication, pp. 1–36.
Naish, T.R., Kamp, P.J.J., 1997a. Sequence stratigraphy of sixth-order (41 k.y.) Pliocene-Pleistocene cyclothems, Wanganui basin, New Zealand: a case for the regressive systems tract. GSA Bull. 109, 978–999.
Naish, T., Kamp, P.J.J., 1997b. Foraminiferal depth palaeoecology of Late Pliocene shelf sequences and system tracts, Wanganui Basin, New Zealand. Sediment. Geol. 110, 237–255.
Naish, T.R., Wehland, F., Wilson, G.S., Browne, G.H., Cook, R.A., Morgans, H.E.G., Rosenberg, M., King, P.R., Smale, D., Nelson, C.S., Kamp, P.J.J., Ricketts, B., 2005. An integrated sequence stratigraphic, palaeoenvironmental, and chronostratigraphic analysis of the Tangahoe Formation, southern Taranaki coast, with implications for mid-Pliocene (c. 3.4-3.0 Ma) glacio-eustatic sea-level changes. J. Roy. Soc. N. Z. 35, 151–196.
Playter, T., Corlett, H., Konhauser, K., Robbins, L., Rohais, S., Crombez, V., MacCormack, K., Rokosh, D., Prenoslo, D., Furlong, C.M., Pawlowicz, J., Gingras, M., Lalonde, S., Lyster, S., Zonneveld, J.-P., 2018. Clinoform identification and correlation in fine-grained sediments: a case study using the Triassic Montney Formation. Sedimentology 65, 263–302.
Posamentier, H.W., Jervey, M.T., Vail, P.R., 1988. Eustatic controls on clastic deposition, I: conceptual framework. In: Wilgus, C.K., Hastings, B.S., Kendall, C.G.StC., Posamentier, H.W., Ross, C.A., Van Wagoner, J.C. (Eds.), Sea Level Changes: an Integrated Approach, vol. 42. SEPM Special Publication, pp. 110–124.
Posamentier, H.W., Allen, G.P., 1999. Siliciclastic sequence stratigraphy – concepts and applications. SEPM Concepts Sedimentol. Paleontol. 7, 210.
Ratcliffe, K.T., Wright, A.M., Schmidt, K., 2012. Application of inorganic whole–rock geochemistry to shale resource plays: an example from the Eagle Ford Shale Formation, Texas. Sediment. Rec. 10, 4–9.
Reijenstein, H.M., Posamentier, H.W., Bande, A., Lozano, F.A., Dominguez, R.F., Wilson, R., Catuneanu, O., Galeazzi, S., 2020. Seismic geomorphology, depositional elements, and clinoform sedimentary processes: impact on unconventional reservoir prediction. In: Minisini, D., Fantin, M., Lanusse Noguera, I., Leanza, H.A. (Eds.), Integrated Geology of Unconventionals: the Case of the Vaca Muerta Play, vol. 121. AAPG Memoir, Argentina, pp. 237–266.
Sano, J.L., Ratcliffe, K.T., Spain, D.R., 2013. Chemostratigraphy of the haynesville shale. In: Hammes, U., Gales, J. (Eds.), Geology of the Haynesville Gas Shale in East Texas and West Louisiana,, U.S.A., vol. 105. AAPG Memoir, pp. 137–154.
Siggerud, E.I.H., Steel, R.J., 1999. Architecture and trace-fossil characteristics of a 10,000e20,000 year, fluvial-to-marine sequence, SE Ebro Basin, Spain. J. Sediment. Res. 69, 365–383.
Taylor, K.G., Gawthorpe, R.L., Van Wagoner, J.C., 1995. Stratigraphic control on laterally persistent cementation. Book Cliff, Utah. J. Geol. Soc. 152, 225–228.
Taylor, K.G., Gawthorpe, R.L., Curtis, C.D., Marshall, J.D., Awwiller, D.N., 2000. Carbonate cementation in a sequence-stratigraphic framework: upper cretaceous sandstones, book cliffs, Utah-Colorado. J. Sediment. Res. 70, 360–372.
Turner, B.W., Tréanton, J.A., Slatt, R.M., 2016. The use of chemostratigraphy to refine ambiguous sequence stratigraphic correlations in marine mudrocks. An example from the Woodford Shale, Oklahoma, USA. J. Geol. Soc. 173, 854–868.
Van Wagoner, J.C., Posamentier, H.W., Mitchum, R.M., Vail, P.R., Sarg, J.F., Loutit, T.S., Hardenbol, J., 1988. An overview of the fundamentals of sequence stratigraphy and key definitions. In: Wilgus, C.K., Hastings, B.S., Kendall, C.G.StC., Posamentier, H. W., Ross, C.A., Van Wagoner, J.C. (Eds.), Sea Level Changes: an Integrated Approach, vol. 42. SEPM Special Publication, pp. 39–45.
Vecsei, A., Duringer, P., 2003. Sequence stratigraphy of Middle Triassic carbonates and terrigenous deposits (Muschelkalk and Lower Keuper) in the SW Germanic Basin: maximum flooding versus maximum depth in intracratonic basins. Sediment. Geol. 160, 81–105.
Zecchin, M., Caffau, M., 2012. The vertical compartmentalization of reservoirs: an example from a outcrop analog, Crotone Basin, southern Italy. AAPG (Am. Assoc. Pet. Geol.) Bull. 96, 155–175.
Zecchin, M., Catuneanu, O., 2013. High-resolution sequence stratigraphy of clastic shelves I: units and bounding surfaces. Mar. Petrol. Geol. 39, 1–25.
Zecchin, M., Catuneanu, O., 2015. High-resolution sequence stratigraphy of clastic shelves III: applications to reservoir geology. Mar. Petrol. Geol. 62, 161–175.
Zecchin, M., Catuneanu, O., Rebesco, M., 2015. High-resolution sequence stratigraphy of clastic shelves IV: high-latitude settings. Mar. Petrol. Geol. 68, 427–437.
Zecchin, M., Catuneanu, O., 2017. High-resolution sequence stratigraphy of clastic shelves VI: mixed siliciclastic-carbonate systems. Mar. Petrol. Geol. 88, 712–723.
Zecchin, M., Catuneanu, O., Caffau, M., 2017. High-resolution sequence stratigraphy of clastic shelves V: criteria to discriminate between stratigraphic sequences and sedimentological cycles. Mar. Petrol. Geol. 85, 259–271.
Zecchin, M., Catuneanu, O., 2020. High-resolution sequence stratigraphy of clastic shelves VII: 3D variability of stacking patterns. Mar. Petrol. Geol. 121, 104582.
Zecchin, M., Caffau, M., Catuneanu, O., 2021. Recognizing maximum flooding surfaces in shallow-water deposits: an integrated sedimentological and micropaleontological approach (Crotone Basin, southern Italy). Mar. Petrol. Geol. 133, 105225.
Zecchin, M., Caffau, M., Catuneanu, O., 2022a. Identification of maximum flooding surfaces at different scales: the case of the piacenzian to gelasian cutro clay and strongoli sandstone (Crotone Basin, southern Italy). Mar. Petrol. Geol. 146, 105971.
Zecchin, M., Catuneanu, O., Caffau, M., 2022b. High-resolution sequence stratigraphy of clastic shelves VIII: full-cycle subaerial unconformities. Mar. Petrol. Geol. 135, 105425.